A Unified Electron Transfer Model for the Different Precursors and Excited States of the Hydrated Electron

Tak W. Kee, Dong Hee Son, Patanjali Kambhampati, and Paul F. Barbara*

Department of Chemistry and Biochemistry, The University of Texas at Austin, Austin, Texas 78712

Received: December 15, 2000; In Final Form: June 18, 2001

Femtosecond spectroscopy measurements are reported on the electron transfer, ET, reactions of the precursor states of the hydrated electron in the multiphoton ionization of water and the single-photon ionization of $Fe(CN)_6^{4-}$ in aqueous solutions. The ET reaction corresponds to an electron scavenging by various electron acceptors, such as Cd^{2+}. Using the data reported herein, and previously published data on the scavenging kinetics of other electron precursors (e.g., from radiolysis) and optically excited states of the hydrated electron, it was shown that the rate constant of ET varies inversely with the volume of specific form of the hydrated electron. These data strongly support a unified model for the electron-transfer kinetics of many forms of delocalized electrons with localized electron acceptors in which ET rates are assumed to be proportional to the average electron density of the specific hydrated electron excited state or precursor.

I. Introduction

The hydrated electron, an excess electron in water, is a fundamental species in radiation- chemistry,[1,2] biology,[3,4] and physics.[5] It is also a critical intermediate in the photoionization of aqueous solutions and other charge-transfer processes in water. The equilibrated form of the hydrated electron, e_{eq}, has a microsecond lifetime in the absence of electron scavengers and at low e_{eq} concentration. The e_{eq} has an s-orbital like electronic wave function. It is localized, trapped, and solvated in a cavity with a radius of ∼3 Å that is surrounded by ∼6 water molecules.[6] Not surprisingly, e_{eq} is a strong reducing agent and it irreversibly reacts with oxidants (Cd^{2+}, SeO_4^{2-}, NO_3^-, etc) by an electron transfer (ET) process, e.g.

$$e_{eq} + NO_3^- \xrightarrow{k_{ET}} NO_3^{2-} \qquad (1)$$

This process, which is commonly referred to as "scavenging," occurs at a diffusion controlled rate for many scavengers.[7] The kinetics of e_{eq} are typically measured by probing the broad electronic absorption band of e_{eq}, which is peaked at 720 nm.

Besides the ground state, e_{eq}, there are a number of high energy, highly delocalized forms of the hydrated electron that have lifetimes in the range of 50−300 fs.[8−12] These species (Figure 1) can be divided into two groups: namely; (i) optically excited states of the equilibrated hydrated electron (e_p and $e_{CB'}$) and (ii) various "precursor states" of the hydrated electron ($e_{CB''}$, H_2O^*, and H_2O^{**}). It is noteworthy that the largest forms of the hydrated electron, $e_{CB'}$ and $e_{CB''}$, are the so-called conduction band electrons. They have radii (Gaussian distribution width, σ) over 30 Å.[13,14] These short-lived (50−100 fs) states encompass thousands of water molecules. The precursor states are involved in the common strategies for producing e_{eq} which includes the following: (i) radiolysis of water and aqueous solution using ionizing radiation (e.g., 20 MeV electron accelerator beams); (ii) UV multiphoton ionization of water; and (iii) single and multiphoton ionization of electron donors (I^-, $Fe(CN)_6^{4-}$, etc) in an aqueous solution. This paper is concerned with the ET kinetics of the hydrated electron and various nonequilibrium forms of the excess electron in water. With a few exceptions, the ET scavenging kinetics of the species in Figure 1 have previously been measured by a variety of techniques.[7,15,16] In this paper, we measure the ET scavenging kinetics of the missing examples, namely the precursor states H_2O^* and H_2O^{**} of the multiphoton ionization of water at 266 nm (2 photon) and 400 nm (3+1 photons),[17] respectively. We also measure the scavenging kinetics for the precursor state for the single-photon ionization[18] of $Fe(CN)_6^{4-}$ (not shown in Figure 1).

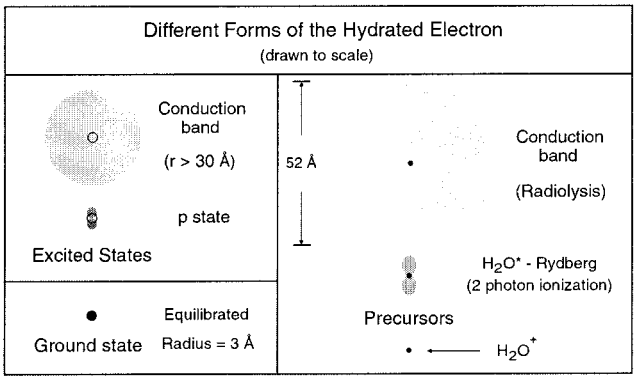

Figure 1. Schematic representation of the different forms of the excess electron in water drawn to scale using the published estimates of the radii of different states, see text and Table 1 for further details. The gray scale in this figure roughly indicates the average relative electron density, i.e., the inverse of "volume" of the wave function. On the left-hand side are the ground and excited states of the hydrated electron. The small circles inside the excited states of the hydrated electron represent the cavity that e_{eq} occupied before being excited. On the right-hand side are the precursors to the hydrated electron. Note that H_2O^+ is located at the center of the precursor states.

The ET kinetics of the hydrated electron and various nonequilibrium forms of the excess electron in water offer insight into an unusual type of ET reaction, i.e., the transfer of

* To whom correspondence should be addressed. E-mail: p.barbara@mail.utexas.edu.

10.1021/jp004516g CCC: $20.00
Published on Web 08/25/2001

a highly diffuse electron donor to a localized electron acceptor. (In contrast, in a typical ET reaction in solution, the electron is transferred between highly localized orbitals on both the donor and the acceptor. Due to the dependence of ET rates on electronic overlap of the donor and acceptor orbitals, direct ET is only rapid over short center-to-center separations (typically < 5 Å)). In this paper, we make the first global analysis of the experimental data on the ET kinetics (scavenging) of the hydrated electron and various nonequilibrium forms of the excess electron in water. This analysis leads to a simple unified model for ET rates of the hydrated electron. The key result of the analysis is that the ET rate constant per scavenger molecule in contact with the hydrated electron, $k_{ET,ps}$, is found to vary inversely with the volume of specific form of the hydrated electron. It is shown that this relationship follows simply from the theoretical expectation that $k_{ET,ps}$ should be proportional to the donor/acceptor electron overlap and correspondingly, the average electron density of the hydrated electron form.

Considering the diversity of the various forms of the excess electron in water, it is useful to review how each form has been produced and investigated.[14−17,19] The left-hand side of Figure 1 displays the optically excited states of the hydrated electron. These states have been prepared by a 3-pulse femtosecond laser sequence involving: (i) a multiphoton ionization pulse to produce e_{eq}; (ii) a near-IR pulse to excite e_{eq}; and (iii) a tunable probe pulse which monitors the absorption of e_{eq} and its excited states. The optically excited states of e_{eq} include a set of three close lying p-orbital like states (prepared by 1 photon excitation), and a higher energy, conduction band $e_{CB'}$ (which is prepared by 2 photon excitation). The lifetimes, radii (σ), and scavenging "yields" for these states have been recently measured by femtosecond spectroscopy, using a novel photosuppression technique for the "geminate reactions" of the hydrated electron with the OH radical and with H_3O^+. These latter species are rapidly produced from fragmentation of the "hole", i.e., H_2O^+.[14,16] The right-hand side of Figure 1 shows the hydrated electron precursor states. These are intermediates in the various methods for preparing e_{eq}. In pulse radiolysis, for example, water or aqueous solution is exposed to ionizing radiation with picosecond time resolution.[20] Water is ionized in a complex, high energy process which involves the production of conduction band electrons, $e_{CB''}$. The spatial extent of $e_{CB''}$ in water has been determined by analyzing pulse radiolysis data.[13]

The physical nature of the precursor states for the photoionization of water and electron donors in aqueous solutions is less well established. For example, for the 2 photon 266 nm photoionization of water with femtosecond pulses, the excitation energy is below the conduction band. The spatial extent of the precursor state, H_2O^*, which is the width (σ) of the e_{eq} distribution produced by the ionization, has been determined from the "geminate reactions" that were described above.[14] Although the exact nature of the precursor state is controversial, the experimental results indicate that it is partially bound to its hole but still highly diffuse. It is likely that H_2O^* has a substantial degree of H_2O−Rydberg character.[17,21−23] Similar arguments can be made for the 3+1 photon 400 nm ionization e_{eq} precursor, H_2O^{**}, although this species is at a higher energy and more diffuse.

II. Experiment Section

The experiments were performed with an amplified Ti: sapphire laser system[24,25] producing 35 fs, 300 μJ pulses centered at 800 nm at a repetition rate of 1 kHz. A portion of the output from the multipass amplifier was frequency doubled in a 300 micron β-barium borate (BBO) crystal to produce the 400 nm photoionization pulses. For the 266 nm photoionization experiments, the 400 nm light was mixed with another component of 800 nm light in a 100 micron BBO crystal. The remaining portion of the amplified laser fundamental was used to generate the probe pulse ($\lambda_p = 650$ nm), derived from wavelength selected white light continuum. The instrument response functions were 70 and 50 fs fwhm for the 266 and 400 nm photoionization experiments, respectively. The sample solutions were continuously flowed though a 300 micron jet nozzle allowing for pump−probe measurements on fresh solutions for each laser pulse.

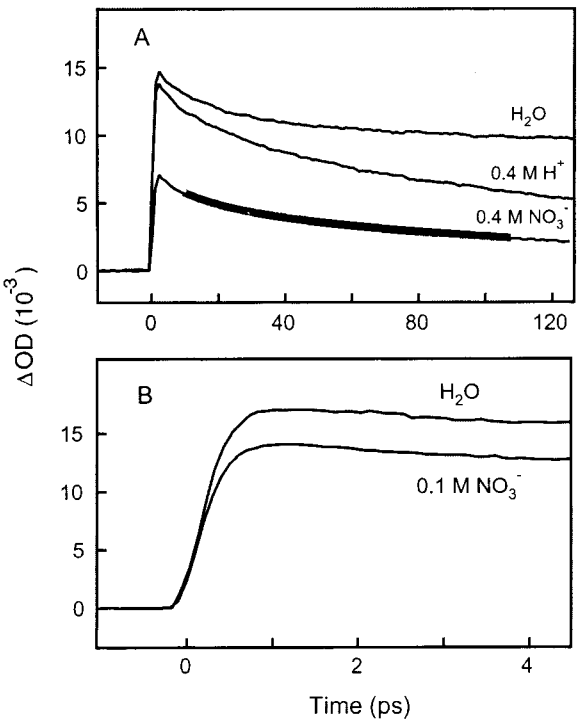

Figure 2. (A) Electron-transfer scavenging kinetic traces of H_2O^*, one of the precursors to the hydrated electron, in 120 ps. The bold curve on the trace of 0.4 M NO_3^- is the calculated trace assuming that the decay in signal is the sum of bimolecular scavenging kinetics of e_{eq} by NO_3^- and geminate processes involving the reaction of the hydrated electron with the OH radical and with H_3O^+. (B) Early time electron-transfer kinetic traces that show that static scavenging occurs on a < 1 ps time scale.

III. Results and Discussion

Photoionization/Scavenging Studies. In this section, we study the ET reactions of the precursor states H_2O^* (266 nm ionization) and H_2O^{**}(400 nm ionization) with various scavengers. The experiments employ ultrafast pump−probe data of e_{eq} as shown in Figure 2, for the 2 photon 266 nm ionization of water and aqueous solutions with scavengers (H^+ and NO_3^-). The neat H_2O data (Figure 2A and 2B) show the expected rise of the absorption of the 650 nm probe light on the hundreds of fs time scale due to the generation of e_{eq} from relaxation of the initially formed H_2O^* precursor state. It is estimated that H_2O^* has a lifetime in the 50−100 fs range.[22,26] The partial decay component of the e_{eq} absorption on the 10−100 ps time scale is due to reaction of the hydrated electron with the OH radical and with H_3O^+. The recombination kinetics have been shown to be well modeled by e_{eq}/hole mutual diffusion and recombination involving an initial distribution of e_{eq}/hole separation with a σ of 12 Å.[14,17] As mentioned in the Introduction, this size can be used as an estimate of the spatial extent of H_2O^*.

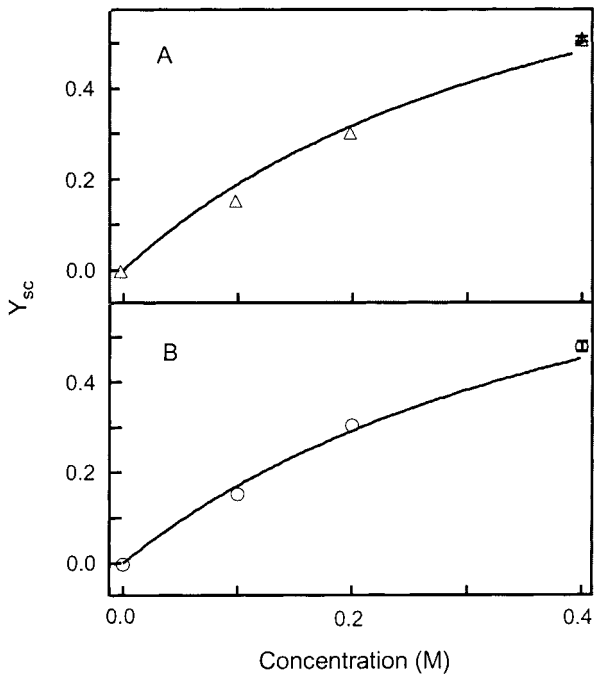

Figure 3. (A) Concentration dependence of the fractional yield (Y_{sc}) of NO_3^- scavenging of H_2O^* and (B) the precursor to the hydrated electron generated from $Fe(CN)_6^{4-}$ with superimposed lines from a fit of eq 2, for both electron precursors.

Figure 2A includes pump−probe transients for H_2O with H^+ and NO_3^- added, i.e., two well-known electron scavengers. The addition of H^+ does very little to the initial (time ≤ 500 fs) absorption of e_{eq} but during the 120 ps transient, an obvious additional decay component is observed due to the rapid bimolecular reaction ($k_{2,s} = 2.4 \times 10^{10}\ s^{-1}\ M^{-1}$) of H^+ with e_{eq}.[27] The extremely small change in the initial e_{eq} absorption implies that the precursor state H_2O^* is not substantially scavenged by H^+. This is not surprising because it has already been shown that H^+ is not an efficient scavenger of other diffuse forms of the excess electron in water, including e_p,[16] $e_{CB'}$,[16] and $e_{CB''}$.[27] The curve in Figure 2A for 0.4 M NO_3^- reveals a large decrease in the initial yield of e_{eq}, which we ascribe to the scavenging of H_2O^*. Considering the short (50−100 fs) lifetime of H_2O^*, this initial scavenging process must occur with essentially no diffusion of NO_3^-. Thus, the H_2O^*/NO_3^- is an example of static scavenging. The static scavenging yields observed for NO_3^- in this paper are similar to the previously reported scavenging yields of e_p, $e_{CB'}$, and $e_{CB''}$ as discussed in detail below.[16,19] The rapid time scale for the static scavenging by NO_3^- is emphasized by Figure 2B, which shows that the initial drop in e_{eq} yield occurs within the formation time of H_2O^*. Furthermore, the slower decay of e_{eq} on the tens of picosecond time scale in the presence of NO_3^- is quantitatively consistent with the simulated decay (thick-line in Figure 2A) based on the sum of independent *bimolecular scavenging* by NO_3^- the reaction of the hydrated electron with the OH radical and with H_3O^+. The nonscavenging component of the dynamics was measured independently using the H_2O only data in Figure 2A. The bimolecular scavenging of NO_3^- was measured nearly independently by examining the NO_3^- decay in experiments with 400 nm photoionization, for which the reaction of the hydrated electron with the OH radical and with H_3O^+ is relatively inefficient due to a large initial electron/hole separation.[14,17]

Figure 3A shows that the observed fractional yield of scavenging, Y_{sc}, of H_2O^* by NO_3^- follows the typical empirical static scavenging behavior

$$Y_{sc} = \frac{C_s[S]}{(C_s[S] + 1)} \qquad (2)$$

where C_s is an empirical scavenging coefficient and [S] is concentration of the scavenger in moles/L. Table 1 shows C_s for H_2O^* and H_2O^{**} from this work, and other forms of the excess electron in water from other references. One important trend in Table 1 is that the scavenging coefficients for the different forms of the excess electron in water and different scavengers are quite similar, within a factor of 2 in nearly all cases. Additionally, different scavengers tend to have very similar Y_{sc} for a specific form of the hydrated electron, especially for the measurements recorded with femtosecond time resolution. The femtosecond data are less distorted by scavenging from subsequent states produced during the rapid relaxation of the precursor or excited states under investigation. Not shown in Table 1 are the scavenging data of H^+. But as mentioned above, H^+ is not an efficient scavenger for the photoexcited and precursor states. (It does efficiently scavenge e_{eq}, although at a slower than diffusion controlled rate).[28,29] Incidentally, previous experiments on hydrated electron scavenging have confirmed that the counterions Na^+ and ClO_4^- are weak scavengers of hydrated electron excited states and precursors.[30,31]

TABLE 1: Electron Transfer Scavenging Kinetics Parameters for the Hydrated Electron and Various Nonequilibrium Forms of the Excess Electron in Water

e form	scavenger	r_{EC}(Å)[a]	C_s[b]	Y_{sc}[c]
e_{eq}		5.0	0.27	0.0265
e_p	NO_3^-	8.7	1.11	0.10
	Cd^{2+}	8.33	1.24	0.11
	SeO_4^{2-}	9.28	0.99	0.09
$e_{CB'}$	NO_3^-	32.0	2.20	0.18
	Cd^{2+}	31.6	2.66	0.21
	SeO_4^{2-}	32.6	1.90	0.16
$e_{CB''}$	NO_3^-	54.0	1.08	0.097
	Cd^{2+}	53.6	0.67	0.063
	SeO_4^{2-}	54.6	2.40	0.194
H_2O^*	NO_3^-	14.0	2.33	0.153
	Cd^{2+}	13.6	1.93	0.162
	SeO_4^{2-}	14.6	2.14	0.176
H_2O^{**}	NO_3^-	22.0	2.38	0.192

[a] $r_{EC} = r_{ex} + r_{sc}$.[7] [b] C_s for H_2O^* is obtained by fitting the data shown in Figure 3A with eq 2. For e_{eq}, e_p, $e_{CB'}$, and H_2O^{**}, C_s is obtained by solving eq 2 with [S] = 0.1 mole/L and the observed Y_{sc}.[16] For $e_{CB''}$, $C_s = k_{pre}\tau_{pre}$, with k_{pre} and τ_{pre} from ref 7. [c] Y_{sc} for [S] = 0.1 mole/L. Y_{sc} for e_{eq} is calculated with eq 3 assuming "perfect" static scavenging, i.e., $k_{ET,ps} \gg 1/\tau$. Here, τ represents an arbitrary time period much shorter than the time-scale for the relative diffusion of e_{eq} and the scavenger. Y_{sc} is obtained from ref 16 for e_p and $e_{CB'}$ and ref 7 for $e_{CB''}$.

We have also investigated scavenging of the precursor state of e_{eq} as generated by the 1 photon ionization of $Fe(CN)_6^{4-}$ with 266 nm pulses. The optical density transients of e_{eq} in H_2O and $Fe(CN)_6^{4-}$ at the same pulse energy (0.8 μJ) are shown in Figure 4. The pulse energy dependence of the H_2O only data is quadratic in pulse energy as expected for a 2 photon ionization process (see inset in Figure 4). In contrast, the e_{eq} signal in $Fe(CN)_6^{4-}$ solution shows a linear power dependence, indicating a 1 photon ionization process, as described previously.[18] Figure 3B shows that the $Fe(CN)_6^{4-}$ precursor state of e_{eq} is also efficiently scavenged by NO_3^- with $Y_{sc} = 0.15$, which is identical to Y_{sc} of H_2O^* within experimental error.

Electron/Scavenger "Encounter Complex" Analysis of the Static Scavenging Yield Data. Following the usual treatment for static scavenging,[7] we introduce the concept of e_x/scavenger

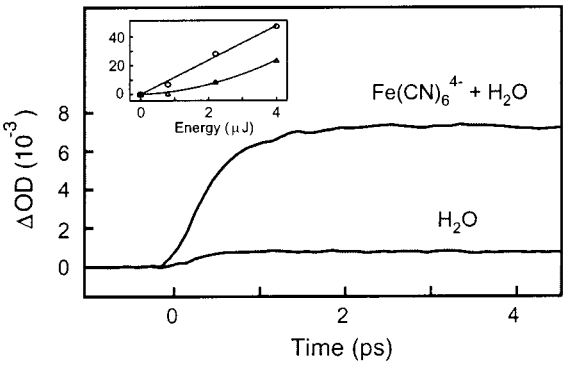

Figure 4. Kinetic traces of the photogenerated hydrated electron in 0.1 M $Fe(CN)_6^{4-}$ aqueous solution. The H_2O only background signal is ~12 times smaller. In the inset, the pulse energy dependence of the signals from 0.1 M $Fe(CN)_6^{4-}$ aqueous solution (○) and H_2O (△) is shown.

"encounter complex," where e_x signifies one of the excess electron forms, i.e., e_p, $e_{CB'}$, $e_{CB''}$, H_2O^* or H_2O^{**}. The radius of this complex, r_{EC}, is assumed to be the sum of the spatial extent, r_x, of the hydrated electron state and radius of the scavenger, r_{sc}.[7] For the larger excess electron forms, e.g. $e_{CB'}$, $r_x \gg r_{sc}$ and $r_{EC} \approx r_x$. The encounter complex may contain 0, 1, 2, ..., or N_s number of scavengers. We assume a single average electron-transfer rate constant per scavenger, $k_{ET,ps}$, if the scavenger is located within the encounter radius, r_{EC}. The ET rate constant per scavenger is assumed to be zero if it is separated by a distance larger than r_{EC} from the center of the hydrated electron. (A more detailed treatment could explicitly treat the radial dependence of the electron density and $k_{ET,ps}$. However, the basic conclusions of this paper would be the same if the more detailed model were employed).

In terms of the encounter complex model for static scavenging, the scavenging yield for a specific hydrated electron form is as follows

$$Y_{sc} = \sum_{i=1}^{\infty} \frac{i k_{ET,ps} f_i}{(i k_{ET,ps} + 1/\tau)} \tag{3}$$

where each i^{th} term in the sum corresponds to an encounter complex with i scavengers; τ is the lifetime of the hydrated electron state; and f_i is the fraction of electrons complexed with i scavengers. Although reliable values of τ are not available for all of the various states, most of the states are believed to have a lifetime in the range of 50−100 fs.[11,26,32] An exception is the p state, which is reported to have a lifetime of 300 fs.[16,32,33]

The simplest expectation for f_i is the Poisson distribution, as follows

$$f_i = \frac{\bar{N}_s{}^i \, e^{-\bar{N}_s}}{i!} \tag{4}$$

where $\bar{N}_s$ is the mean number of scavengers in the volume of the encounter complex, V_{EC}

$$V_{EC} = (4/3)\,\pi\, r_{EC}{}^3 \tag{5}$$

and $\bar{N}_s$ is simply given by

$$\bar{N}_s = 1000[S] L_A V_{EC} \tag{6}$$

where [S] is the concentration of the scavenger in moles/L, L_A is Avogadro's number, and V_{EC} is in m^3.

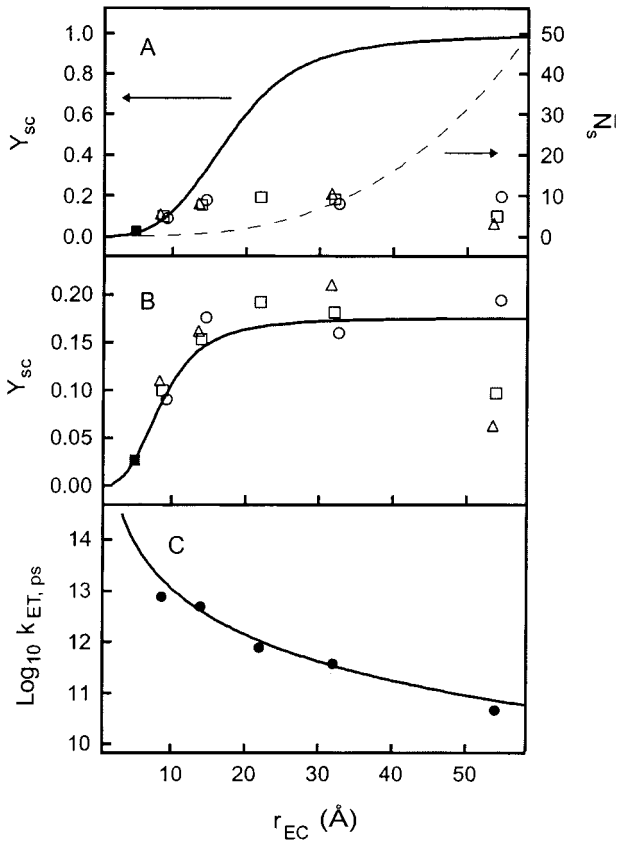

Figure 5. Experimental Y_{sc} of NO_3^-, Cd^{2+}, and SeO_4^{2-} are represented as □, △, and ○ respectively. (A) The solid line is calculated with eq 3 assuming that $k_{ET,ps}$ as a constant (1.6×10^{13} s^{-1}). The dash line shows $\bar{N}_s$ as a function of r_{EC}. (B) Y_{sc} is plotted as a function of r_{EC} assuming that $k_{ET,ps}$ is proportional to the inverse of $r_{EC}{}^3$ (see eq 10). (C) Plot (data points) of the logarithm of the average $k_{ET,ps}$ as a function of r_{EC} for each form of the hydrated electron (solved from eq 3 using the experimental scavenging yield data). The theoretical line in (C) is eq 10 using a best-fit value for the single adjustable parameter, i.e., $k_{ET,ps}{}^o = 9.02 \times 10^{13}$ s^{-1}.

It is interesting to consider typical values of f_i and $\bar{N}_s$ for the various scavenging experiments on the hydrated electron, see Table 1. For reference, we use [S] = 0.1 mol/L. Figure 5A shows the observed Y_{sc} values (points) for the different forms vs r_{EC} for each state and various scavengers. Superimposed on these data is a plot of $\bar{N}_s$ vs r_{EC}. For the p state electron, $\bar{N}_s = 0.17$ and only the encounter complex with one scavenger is relevant in the scavenging process. In this limit

$$Y_{sc} = \frac{k_{ET,ps} \cdot f_i}{(k_{ET,ps} + 1/\tau)} \tag{7}$$

In contrast for $e_{CB'}$, $\bar{N}_s = 8.26$. For such a larger $\bar{N}_s$, the scavenging yield is approximately

$$Y_{sc} = \frac{\bar{N}_s \cdot k_{ET,ps}}{(\bar{N}_s \cdot k_{ET,ps} + 1/\tau)} \tag{8}$$

Comparing these two limits reveals that if $k_{ET,ps}$ was the same for the p state and conduction band, the latter should have been much more efficiently scavenged. This is emphasized by the theoretical Y_{sc} line (Figure 5A) corresponding to eq 3, calculated by using $k_{ET,ps} = 1.6 \times 10^{13}$ s^{-1}, the reported value[16] for NO_3^- scavenging of e_p and a fixed e_x lifetime of $\tau = 75$ fs. Note that this line predicts a large increase in Y_{sc} with r_{EC} and in particular nearly unity scavenging of the conduction band. In fact, neither

prediction is supported by the experimental data. Thus, $k_{ET,ps}$ is clearly not identical for different forms.

It is interesting to consider how $k_{ET,ps}$ would be expected to vary with r_{EC} and scavenger according to the theory of electron transfer. In the nonadiabatic theory of electron transfer, the rate constant of ET in a donor/acceptor complex is given by

$$k_{ET} = \frac{2\pi}{\hbar} H_{DA}{}^2 \,\mathrm{DWFC} \tag{9}$$

where H_{DA} is the donor/acceptor electron matrix element and DWFC is the density of states weighted Franck−Condon factor.[34] For electron scavenging of the excited states of e_{eq}, the reaction is probably barrierless, and close to being at the "peak of the Marcus parabola" due to the high exoergicity of these reactions and the availability of open electronic and vibrational channels involving excited states of the scavenger. Thus, DWFC may be similar for the various scavengers. Indeed, the scavenging yields Y_{sc} for a particular hydrated electron form for the different "good" scavengers tend to be very similar. For example, Y_{sc} of H_2O^* are identical within experimental error for NO_3^-, Cd^{2+}, and SeO_4^{2-}. This is consistent with the barrierless limit because the scavenging rates do not vary with the reduction potential of the different acceptors. (An exception to this trend is the radiolysis results, where the Y_{sc} of e_{CB}″ values vary over a larger range. The variation in the radiolysis results with the different scavengers may partly be in error due to complications from dynamic scavenging of e_{eq}, which is a factor due to the slower time resolution of the pulsed radiolysis measurements.[7,15] Although the radiolysis results are corrected for dynamic scavenging, the correction process may still have errors).

The key to understanding the r_{EC} dependence of $k_{ET,ps}$ is that H_{DA} is proportional to the overlap of the donor/acceptor orbitals. This implies that in the case of an overlap of a diffuse e_x orbital with a localized ~1 Å acceptor orbital, the *average* $k_{ET,ps}$ should be proportional to the *average electron density* of e_x. Correspondingly, $k_{ET,ps}$ should be inversely proportional to the volume ($r_x{}^3$) of e_x, as shown in eq 10

$$k_{ET,ps} = \frac{k^o_{ET,ps} r_{e_{eq}}{}^3}{r_x{}^3} \tag{10}$$

Here, $k^o_{ET,ps}$ is a constant that is arbitrarily assigned to static scavenging rate constant for e_{eq}. Figure 5B compares the predicted Y_{sc} values from eq 3 using $k_{ET,ps}$ predicted by eq 10. *The qualitative agreement with experiment strongly suggests that $k_{ET,ps}$ does in fact decrease inversely with volume of the hydrated electron state.* The required $k_{ET,ps}{}^o$ value was obtained by fitting the combination of eqs 3 and 10 to the Y_{sc} values. The best-fit value for $k_{ET,ps}{}^o$ falls in the range of $0.5-1.0 \times 10^{14}$ s^{-1}. For the theoretical line in Figure 5B, the only other required parameters are $\tau = 75$ fs(assumed) and the previously estimated r_{EC} values (see Table 1). Apparently, the $Fe(CN)_6{}^{4-}$ precursor state of e_{eq} is also well described by eq 10 because Y_{sc} for this precursor is similar to the other values. Unfortunately, no estimate for r_x for $Fe(CN)_6{}^{4-}$ is available and the scavenging results for $Fe(CN)_6{}^{4-}$ are not included in Figure 5.

The extent to which this simple relationship (eq 10) is the major factor determining $k_{ET,ps}$ for the various forms of excess electron in water with good scavengers is dramatically demonstrated in Figure 5C. Here, experimental estimates (points) for $k_{ET,ps}$ have been *calculated by solving eq 3 for $k_{ET,ps}$* using the observed Y_{sc} and r_{EC} for each state. The known lifetime of $\tau = 300$ fs was used for e_p and a lifetime of $\tau = 75$ fs was used for the other forms. It is important to emphasize that the $k_{ET,ps}$ data points in Figure 5C were calculated without assuming any physical dependence of $k_{ET,ps}$ on r_x. The experimentally determined $k_{ET,ps}$ values do agree extremely well with the theoretical curve predicted by eq 10. It is particularly interesting that the ET kinetics of the diverse set of excess electron forms in Figure 1 can be explained by a simple unified treatment. The single adjustable parameter for the theoretical line in Figure 5C is $k^o_{ET,ps}$, the scavenging rate constant for the reaction of the localized s state, e_{eq}, with a localized acceptor. The best-fit value ($k^o_{ET,ps} = 9.02 \times 10^{13}$ s^{-1}) is similar to the reported measurements from other examples of barrierless ET reactions between closely spaced, localized donors and acceptors, for instance the intramolecular ET reactions of metal−metal mixed valence compounds with small bridging ligands.[35,36]

IV. Conclusion and Summary

We have measured the electron-transfer scavenging kinetics of the precursor states of the UV multiphoton ionization of water and the single-photon ionization of $Fe(CN)_6{}^{4-}$ with various electron scavengers. The analysis of these data, and other previously published data on the scavenging yields of other electron precursor and hydrated electron excited states, leads to a simple unified model for ET rates of the hydrated electron. The key result of the analysis is that the ET rate constant per scavenger molecule in contact with the hydrated electron, $k_{ET,ps}$, is found to vary inversely with the volume of specific form of the hydrated electron. It is shown that this relationship follows simply from the theoretical expectation that $k_{ET,ps}$ should be proportional to the donor/acceptor electron overlap and correspondingly, the average electron density of the hydrated electron form.

Acknowledgment. We gratefully acknowledge support of this research by the Basic Energy Sciences Program of the Department of Energy and the Robert A. Welch Foundation. We thank S. M. Pimblott, D. M. Bartels, P. J. Rossky, J. A. LaVerne, and C. D Jonah for helpful discussions.

References and Notes

(1) Spinks, J. W. T.; Woods, R. J. *An Introduction to Radiation Chemistry*; John Wiley & Sons: New York, 1976.

(2) Mozumder, A. *Fundamentals of Radiation Chemistry*; Academic Press: London, 2000.

(3) Coggle, J. E. *Biological Effects of Radiation*; International Publications Service, Taylor & Francis Inc.: New York, 1983.

(4) Pottinger, S. M. A. *Radiation Biology*: *a Textbook*: *General Consideration of Radiation Damage*; Mount Saint Scholastica College, Tape Institute: Atchison, Kansas, 1962.

(5) Dyson, N. A. *Radiation Physics with Applications in Medicine and Biology*; E. Horwood: New York, 1993.

(6) Prezhdo, O. V.; Rossky, P. J. *J. Phys. Chem.* **1996**, *100*, 17094−17102.

(7) Pimblott, S. M.; LaVerne, J. A. *J. Phys. Chem. A* **1998**, *102*, 2967−2975.

(8) Migus, A.; Gauduel, Y.; Martin, J. L.; Antonetti, A. *Phys. Rev. Lett.* **1987**, *58*, 1559−1562.

(9) Long, F. H.; Lu, H.; Eisenthal, K. B. *Phys. Rev. Lett.* **1990**, *64*, 1469−1475.

(10) Long, F. H.; Lu, H.; Shi, X.; Eisenthal, K. B. *Chem. Phys. Lett.* **1991**, *185*, 47−51.

(11) Yokoyama, K.; Silva, C.; Son, D. H.; Walhout, P. K.; Barbara, P. F. *J. Phys. Chem. A* **1998**, *102*, 6957−6966.

(12) Silva, C.; Walhout, P. K.; Yokoyama, K.; Barbara, P. F. *Phys. Rev. Lett.* **1998**, *80*, 1086−1089.

(13) Pimblott, S. M.; LaVerne, J. A. *J. Phys. Chem.* **1997**, *101*, 5828−5838.

(14) Kambhampati, P.; Son, D. H.; Kee, T. W.; Barbara, P. F. *J. Phys. Chem. A* **2000**, submitted.

(15) Jonah, C. D.; Miller, J. R.; Matheson, M. S. *J. Phys. Chem.* **1977**, *81*, 1618−1622.

(16) Son, D. H.; Kambhampati, P.; Kee, T. W.; Barbara, P. F. *J. Am. Chem. Soc.* **2000**, submitted.

(17) Crowell, R. A.; Bartels, D. M. *J. Phys. Chem.* **1996**, *100*, 17 940−17 949.

(18) Pommeret, S.; Naskrecki, R.; Meulen, P. v. d.; Ménard, M.; Vigneron, G.; Gustavsson, T. *Chem. Phys. Lett.* **1998**, *288*, 833−840.

(19) Pastina, B.; LaVerne, J. A.; Pimblott, A. M. *J. Phys. Chem. A* **1999**, *103*, 5841−5846.

(20) Jonah, C. D.; Matheson, M. S.; Miller, J. R.; Hart, E. J. *J. Phys. Chem.* **1976**, *80*, 1267−1270.

(21) Sander, M. U.; Luther, K.; Troe, J. *Ber. Bunsen-Ges. Phys. Chem.* **1993**, *97*, 953.

(22) Sander, M. U.; Gudiksen, M. S.; Luther, K.; Troe, *J. Chem. Phys.* **2000**, *258*, 257−265.

(23) Bartels, D. M.; Crowell, R. A. *J. Phys. Chem.* **2000**, *104*, 3349−3355.

(24) Asaki, M. T.; Huang, C. P.; Garvey, D.; Zhou, J.; Murnane, M. M.; Kapteyn, H. C. *Opt. Lett.* **1993**, *18*, 977.

(25) Backus, S.; Peatross, J.; Huang, C. P.; Kapteyn, H. C.; Murnane, M. M. *Opt. Lett.* **1995**, *20*, 2000.

(26) Vilchiz, V. H.; Kloepfer, J. A.; Germaine, A. C.; Lenchenkov, V. A.; Bradforth, S. E. *J. Phys. Chem. A* **2001**, *105*, 1711.

(27) Shiraishi, H.; Sunaryo, G. R.; Ishigure, K. *J. Phys. Chem. A* **1994**, *98*, 5164−5173.

(28) Goulet, T.; Jay-Gerin, J. P. *J. Chem. Phys.* **1992**, *96*, 5076−5087.

(29) Pimblott, S. M. *J. Phys. Chem.* **1991**, *95*, 6946−6951.

(30) Telser, T.; Schindewolf, U. *J. Phys. Chem.* **1986**, *90*, 5378−5382.

(31) Thomas, J. K.; Gordon, S.; Hart, E. J. *J. Phys. Chem.* **1964**, *68*, 1524−1527.

(32) Keszei, E.; Nagy, S.; Murphrey, T. H.; Rossky, P. J. *J. Chem. Phys.* **1993**, *99*, 2004−2011.

(33) Bittner, E. R.; Rossky, P. J. *J. Chem. Phys.* **1997**, *107*, 8611−8618.

(34) Barbara, P. F.; Meyer, T. J.; Ratner, M. A. *J. Phys. Chem.* **1996**, *100*, 13 148−13 168.

(35) Reid, P. J.; Silva, C.; Barbara, P. F.; Karki, L.; Hupp, J. T. *J. Phys. Chem.* **1995**, *99*, 2609−2616.

(36) Kambhampati, P.; Son, D. H.; Kee, T. W.; Barbara, P. F. *J. Phys. Chem. A* **2000**, *104*, 10 637−10 644.